J Mater Sci (2008) 43:1505–1509
DOI 10.1007/s10853-007-2378-z

Fabrication and characterization of anisotropic dielectrics for low-loss microwave applications

Lanlin Zhang · Gokhan Mumcu · Salih Yarga · Kubilay Sertel · John L. Volakis · Henk Verweij

Received: 3 October 2007 / Accepted: 3 December 2007 / Published online: 1 January 2008

Abstract New magneto-photonic assembly designs for high-gain antennas require dielectrics with a significant anisotropy and low loss at GHz frequencies. This paper describes an approach to fabricate such dielectrics from ceramic laminates. These laminates consist of two ceramics with largely different permittivities and low dielectric losses. Alternating layers of commercially available α-Al_2O_3 and Nd-doped $BaTiO_3$ were laminated using organic adhesives. Equivalent permittivity tensors and loss tangents were characterized using a resonant cavity-based approach, which was coupled with a finite-element method full-wave solver. Measured permittivity values were in good agreement with mean field predictions; a minimum loss tangent 1.1×10^{-3} was obtained when using one-component epoxy (Loctite®-3982) adhesive. Application of two-component epoxy (M-bond 610) adhesive results in a slightly higher loss but better mechanical properties and machinability. These laminates were used to demonstrate high gain in a prototype antenna with 6 misaligned anisotropic dielectric layers.

L. Zhang · H. Verweij (✉)
Group Inorganic Materials Science, Department of Materials Science and Engineering, The Ohio State University, Columbus, OH 43210-1178, USA
e-mail: Verweij@matsceng.ohio-state.edu

G. Mumcu · S. Yarga · K. Sertel · J. L. Volakis
ElectroScience Laboratory, Department of Electrical and Computer Engineering, The Ohio State University, Columbus, OH 43212, USA

Introduction

Metamaterials and engineered artificial media hold the promise to enhance the antenna performance for RF and microwave applications. The recent discovery of the frozen propagation modes in magnetic photonic assemblies (MPAs) was predicted to improve coupling of microwave radiation by significantly slowing down incoming electromagnetic waves, hence increasing field amplitudes within the structure [1, 2]. Computer simulations led to MPA designs with 10–40 unit cells, each made of two anisotropic dielectric (AD) layers and one ferrimagnetic (F) layer [3], providing a 5-fold electric field amplitude increase. To minimize the overall size, individual layers must be $\sim$0.5 mm thin. The dielectric anisotropy of the AD layers must be >2 with very low dielectric losses (ultimately $\tan \delta < 10^{-5}$). This strict low-loss requirement is primarily due to the extremely slow nature of wave propagation associated to the frozen mode. The layers must have relatively large lateral dimensions (>10 mm at X-band) so that the antenna aperture, presented to the incoming wave, is significant (and the MPA design can be based on an infinite aperture).

Single crystal rutile has an intrinsic dielectric anisotropy with $\varepsilon_a = 85$ and $\varepsilon_c = 165$ at GHz frequencies [4]; however, its high cost prohibits practical use, especially in the required cm scales. Therefore, both the dimension and low-loss requirements lead to a choice for mean field AD layers made from ceramic laminates (CLs) [5, 6]. The CLs presented in this paper are made of two diamagnetic ceramics with low $\tan \delta$ and largely different ε_r, alternatively laminated with an adhesive. Slicing of the CLs, perpendicular to the original sheet surfaces, results in a "striped" composite layer with an effective in-plane dielectric anisotropy at microwave frequencies. The two ceramic compositions that lie readily at hand are α-Al_2O_3 with $\varepsilon_r = 10$ and tan $\delta = 2 \times 10^{-5}$ [7] and TiO_2 (rutile phase) with $\varepsilon_r = 100$ and tan $\delta = 6 \times 10^{-5}$ [8]. This choice is based on favorable dielectric (loss) properties, a large difference in ε_r, and the simple chemical composition. Dense α-Al_2O_3 sheets are commercially available as substrates. Since that is not the case for TiO_2, commercially available Nd-doped $BaTiO_3$ substrates were obtained with similar properties. Lamination by co-sintering is not favorable for α-Al_2O_3 and Nd-doped $BaTiO_3$ substrates due to their different thermal expansion coefficients (TEC). As a result, an external adhesive is applied during lamination.

In this paper, the dielectric properties of the laminates are presented and compared with those of single crystal rutile. The use of 1 mm thick AD layers, cut from the optimized CLs, is demonstrated for a prototype high-gain microwave antenna consisting of a 6-layer photonic assembly. Similarly, 1 mm thick AD layers with in-plane rotation were obtained for a 12-layer photonic assembly.

Sample preparation and in-cavity measurements

α-Al_2O_3 (purity 99.6%, $\varepsilon_r = 10$) and Nd-doped $BaTiO_3$ (TD82, $\varepsilon_r = 80$) substrates were obtained from CoorsTek Inc., with dimensions of 50 mm × 50 mm × 50 mm and both surfaces lapped. They were alternatively laminated to the 8- and 15-layer CLs, as shown in Fig. 1, for in-cavity measurement. In concordance with the crystallographic notations for the single crystal rutile (TiO_2) structure, an "*a*-axis" was defined parallel to the original isotropic substrate surface planes and a "*c*-axis" perpendicular to those planes. Adhesives used for lamination included organic double-tape 3M-9942, plastic adhesive 3M-4475, cyanoacrylate Loctite®-401, single-component epoxy Loctite®-3982, and two-component epoxy M-bond 610. The laminates from 28 pieces of α-Al_2O_3 and 28 pieces of TD82 substrates were machined into 1 mm thick layers using diamond cutting and grinding, by Louwers Glass and Ceramic Technologies, the Netherlands. Two rutile crystals were obtained from MTI Corp., with 3 mm × 1.6 mm × 10 mm (*x*–*y*–*z*) dimensions. The crystallographic *c*-axis of the 1st and 2nd rutile samples was along the *y* and *x*-dimensions, respectively.

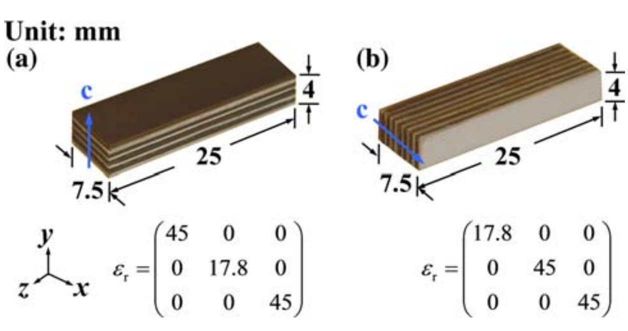

Fig. 1 Sample geometries for dielectric measurements with dielectric tensors. The light and dark layers are α-Al_2O_3 and TD82, respectively

A resonant cavity measurement approach was used to characterize the dielectric loss. The dimensions of the copper cavity (24 mm × 12.8 mm × 80 mm) were chosen so that specific resonant field distributions can be generated with most of the resonant energy concentrated within the sample. The cavity dimensions were 8 times those of the rutile samples and 3.2 times those of the α-Al_2O_3|TD82 CLs.

The rutile samples, with orientation equivalent to that of the CLs, were placed in the center of the cavity to minimize energy dissipation in the walls and hence the loss due to the cavity itself. A network analyzer (Agilent E8362B) was used to determine the resonance frequencies from power reflection coefficient (S_{11}) measurements [9]. The setup was designed so that the first-order resonant modes had electric fields oriented along the largest geometric dimension. This allows for a one-dimensional search to characterize ε_a independently using the 1st rutile sample. The measured resonance frequency was systematically matched to the computed one by varying ε_a used in the finite-element method (FEM). Similarly, the 2nd rutile sample was used to determine ε_c. Modes that did not concentrate inside the sample were excluded from this consideration. ε_a(rutile) = 85 and ε_c(rutile) = 165 were applied as initial parameters in the FEM simulation. The material loss tangent was estimated using [4]

$$Q_u^{-1} = p_{es}^{a} \tan \delta_a + p_{es}^{c} \tan \delta_c + R_s/G \quad (1)$$

where the unloaded Q_u (ratio of stored energy to dissipated energy per cycle) of the cavity system is calculated from S_{11} [9], tan δ_a and tan δ_c are the loss factors along the *a*- and *c*-axes, and R_s is the surface resistivity of the copper cavity. The electric filling ratios p_{es}^{a} and p_{es}^{c} along the *a*- and *c*-axes are computed via FEM using the corrected values for ε_a and ε_c. The geometric factor *G* describes the amount of electric energy concentrated within the samples with respect to the overall energy inside the cavity. For the first modes in the rutile crystals, *G* factors were $\sim 10^4$; hence, tan δ can be determined with an accuracy of 3×10^{-7} (or 3×10^{-5} if the wall loss was not accounted for [10]).

Characterization of the α-Al_2O_3|TD82 CLs was carried out similarly. For these samples, the *G* factor was calculated to be $\sim 10^3$, allowing for the determination of tan δ with an accuracy of 1×10^{-4}. To validate the effective medium model and the dielectric anisotropy of the CLs, the field distributions simulated using the tensors in Fig. 1 were compared with those from a full-wave model using $\varepsilon_r(\alpha\text{-}Al_2O_3) = 10$ and ε_r(TD82) = 80. Both field distributions were nearly identical,

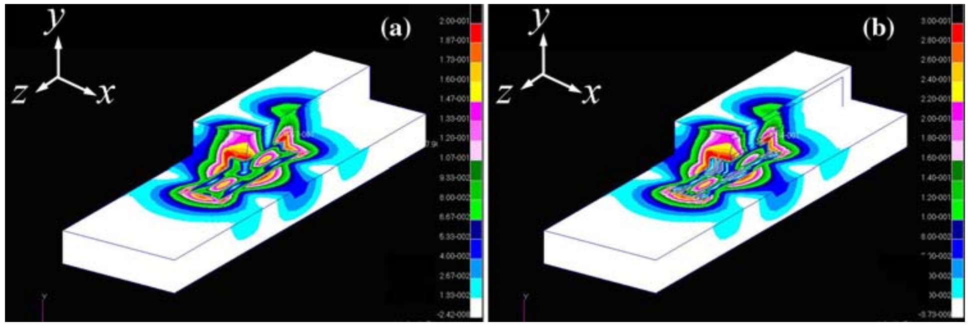

Fig. 2 Field distributions of the resonant mode with the 15-layer CLs at the cavity center, simulated by FEM using: (**a**) effective medium and (**b**) full-wave model. Both calculations were carried out at 7.64 GHz

as shown in Fig. 2 for the sample depicted in Fig. 1b. As expected, measured resonance frequencies of the two CLs were different, confirming their anisotropic dielectric nature.

Loss tangent characterization

The tan δ measurement results for the α-Al_2O_3|TD82 CLs as well as the homogeneous rutile crystals are summarized in Table 1. Theoretical minimum losses in an ideal rutile structure are tan $\delta_a = 7 \times 10^{-10}$ and tan $\delta_c = 4 \times 10^{-10}$ caused by phonon scattering of the microwave field [11]. In a real single crystal, the losses are higher due to imperfections in the crystal lattice, such as interstitials, vacancies, and impurities. Additional losses in the commercial ceramic substrates and adhesive-free α-Al_2O_3|TD82 CLs can be ascribed to

- grain boundaries, porosity, microcracks, and random crystallite orientation [7, 8, 12, 13],
- dangling bonds on the oxide surfaces, which may absorb foreign molecular species, such as water [6],
- oxygen deficiency in TD82, which may result in a higher resistive dissipation due to free electronic charge carriers,
- EM wave reflections at the α-Al_2O_3 and TD82 contact surfaces.

The presence of the external organic adhesives further increased the tan δ values by 1.2 to 3.2× that of the adhesive-free CLs. This extra loss could be explained by the energy dissipation in the organic adhesives and was likely proportional to the overall adhesive volume. The cyanoacrylate Loctite®-401 had a strong adhesion to both α-Al_2O_3 and TD82 substrates, but resulted in the highest loss. As this adhesive is cured by humidity, the water that remained in the adhesive structure may have resulted in additional losses. The adhesive layers were examined using scanning electron microscope (SEM), and their thickness is listed in Table 1. The samples, prepared with fully liquid adhesive (3M-4475 and Loctite®-3982), showed lower losses after pressing to squeeze out superfluous liquid. This confirmed that adhesives should be used as little as possible to minimize the loss. One-component epoxy (Loctite®-3982) with low viscosity and Newtonian behavior, formed very thin adhesive layers under pressure, resulting in the lowest losses. In addition, its heat curing mechanism helped the removal of residual water. SEM analysis revealed a Loctite®-3982 layer of thickness 2.6-4.5 μm from the edges to the center. This thickness is explained by <6 μm deviations of the substrate surfaces from their average flat surface. The losses of the individual substrates: 2.8×10^{-4} for α-Al_2O_3 and 3.7×10^{-4} for TD82 cannot be influenced and limit the minimal loss of the entire CLs. Therefore, commercial ceramic substrates can be used to

Table 1 Estimated dielectric loss in the CLs in comparison with that of rutile single crystal

Material	Loss tan δ	Adhesive layer thickness (μm)	Sustainability to diamond machining
Rutile single crystal	tan $\delta_a = 1.39 \times 10^{-4}$, tan $\delta_c = 1.09 \times 10^{-4}$ at 9.78 GHz	–	–
α-Al_2O_3 substrate	2.8×10^{-4} at 3.37 GHz	–	Yes
TD82 substrate	3.7×10^{-4} at 2.13 GHz	–	Yes
CLs w/o adhesive	0.9×10^{-3} at 7.57 GHz	–	–
CLs w/3M-4475	1.9×10^{-3} at 7.61 GHz	–	No
CLs w/3M-9942	2.6×10^{-3} at 7.67 GHz	~60	No
CLs w/Loctite®-401	2.9×10^{-3} at 7.70 GHz	~15	Yes
CLs w/Loctite®-3982	1.1×10^{-3} at 7.57 GHz	~2.6–4.5	No
CLs w/M-bond 610	1.9×10^{-3} at 7.59 GHz	~5–7	Yes

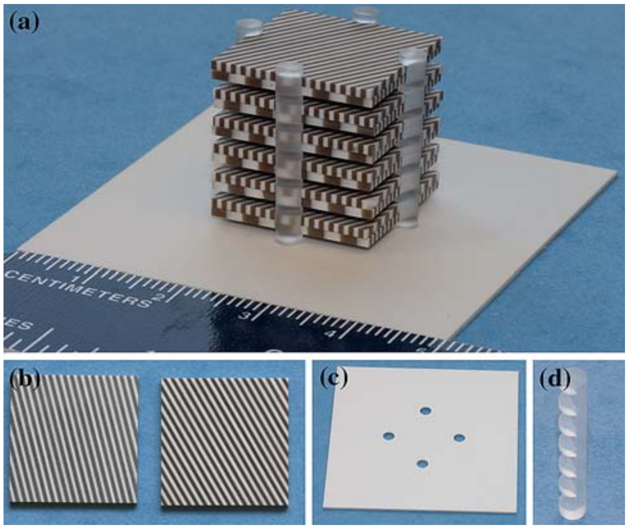

Fig. 3 (**a**) A 12-layer photonic assembly supported in vitreous silica frames onto dense alumina substrate. (**b**) Two AD layers with 15° and 60° in-plane rotation, respectively. (**c**) Dense alumina substrate, with holes drilled to insert vitreous silica frames. (**d**) Vitreous silica frame

demonstrate the feasibility of laminated anisotropic dielectrics, but are not suitable for obtaining $\tan\,\delta < 10^{-5}$.

AD layers, being principal components of the proposed MPA antenna, were obtained by slicing the adhesion-treated CLs into 1 mm thin layers by diamond cutting and grinding. Initial experiments demonstrated the possibility of cutting 0.5 mm thin slices. Layers with larger in-plane dimensions were more difficult to make, because of the limited mechanical strength of TD82. The CLs laminated with 3M-4475, 3M-9942, or Loctite®-3982 could not be machined into large intact layers. Considering the low-loss requirements, the functional AD layers laminated using M-bond 610 were used for a first prototype. AD layers with 15° and 60° in-plane rotation defined with respect to the geometric plane sides, were fabricated with dimensions of 19.1 mm × 19.1 mm × 1.0 mm. The 12-layer photonic

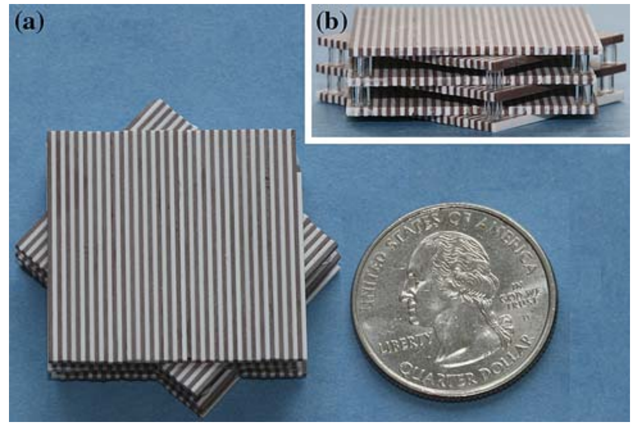

Fig. 4 The 6-layer AD assembly composed of three repeating units: (**a**) top view and (**b**) side view. The transparent spacers are 1.25 mm high quartz tubes

assembly was supported by vitreous silica frames onto a dense alumina substrate, as shown in Fig. 3. Figure 4 shows a simplified assembly of three unit cells, each consisting of two 28.0 mm × 29.0 mm × 1 mm AD layers (AD_1 and AD_2) with 0° in-plane rotation and a 0.25 mm air gap. A relative rotation between AD_1 and AD_2 layers is needed to obtain maximum gain [3]. The optimum rotation angle was determined to be 55°, estimated from FEM simulated gain patterns, and confirmed by experimental patterns. Figure 5 shows simulated and measured far-field gain patterns of the antenna assembly when fed by a slot coupled microstrip line (not shown). These constitute the first measurements of a prototype antenna, based on the extraordinary propagation modes supported by degenerate band edge crystals [3]. Disagreement between the measurements and FEM simulations can be attributed to dielectric losses in the feed structure and the CLs, as well as the external foam used to hold the sample in place during anechoic chamber measurements.

Fig. 5 Measured and simulated gain (dB) patterns of the prototype in Fig. 4: (**a**) *x*–*z* cut and (**b**) *y*–*z* cut

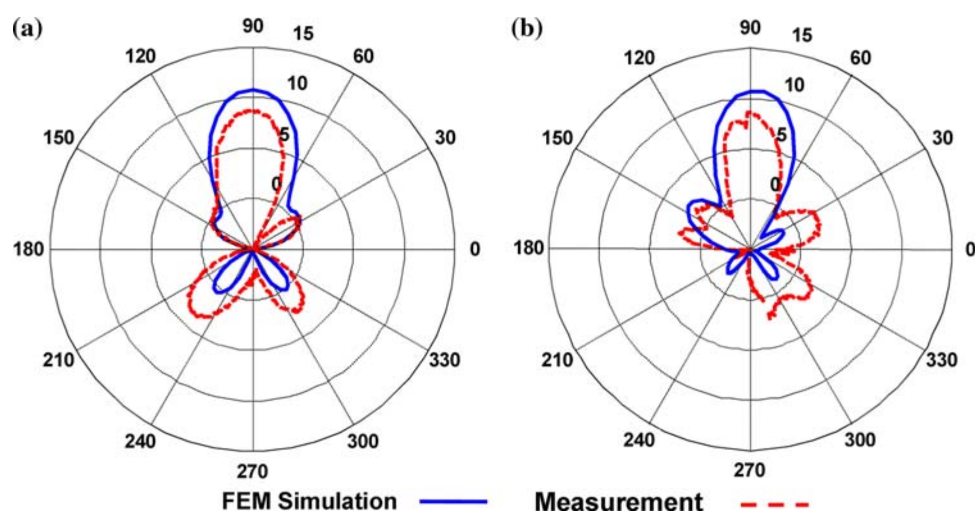

Conclusions

The fabrication and characterization were demonstrated in textured mean-field anisotropic dielectrics from ceramic laminates using commercially available α-Al_2O_3 and Nd-doped $BaTiO_3$ substrates. Loss effects of several possible adhesive agents were documented. Single-component epoxy (Loctite®-3982) was shown to provide fairly low dielectric losses in the GHz range but insufficient machining strength. Two-component epoxy (M-bond 610) provided the best compromise between loss and strength. Artificial anisotropic dielectric layers with thicknesses as small as 0.5 mm were achieved by careful diamond machining. It is shown that 19.1 mm × 19.1 mm × 1.0 mm anisotropic platelets with 15° and 60° in-plane rotation can be made. 28.0 mm × 29.0 mm × 1 mm plates with 0° in-plane rotation were used to demonstrate for the first time in a simplified 6-layer antenna assembly. Future research efforts will focus on optimized ceramic routes to achieve more complete designs and theoretical minimum losses without interference of external adhesion layers.

Acknowledgement This work was supported by the U.S. Air Force Office of Scientific Research under the Grant FA9550-04-1-0359.

References

1. Figotin A, Vitebsky I (2001) Phys Rev E 63:066609
2. Figotin A, Vitebsky I (2003) Phys Rev B 67:165210
3. Mumcu G, Sertel K, Volakis JL, Figotin A, Vitebsky I (2004) IEEE Ante Propagat Soc Symp 2:1395
4. Tobar ME, Krupka J, Ivanov EN, Woode RA (1998) J Appl Phys 83(3):1604
5. Collin RE (1958) IRE Trans Microw Theo Tech 6(2):206
6. Gong X et al (2005) IEEE Trans Micro Theo Tech 53(11):3638
7. Alford NM, Penn SJ (1996) J Appl Phys 80(10):5895
8. Templeton A et al (2000) J Am Ceram Soc 83(1):95
9. Kajfez D, Guillon P (1986) In: Dielectric resonators. Artech House, Inc., Dedham, p 53
10. Krupka J, Derzakowski K, Riddle B, Baker-Jarvis J (1998) Meas Sci Technol 9(10):1751
11. Gurevich VL, Tagantsev AK (1991) Adv Phys 40(6):719
12. Alford NM et al (2001) J Eur Ceram Soc 21:2605
13. Mcneal MP, Jang SJ, Newnham RE (1998) J Appl Phys 83(6):3288